Journal of Alloys and Compounds 506 (2010) 969–972

Contents lists available at ScienceDirect

Journal of Alloys and Compounds

journal homepage: www.elsevier.com/locate/jallcom

Synthesis of CIGS powders: Transition from binary to quaternary crystalline structure

Eunjoo Lee[a,c], Jin Woo Cho[a], Jaehoon Kim[a], Jaeho Yun[b], Jong Hak Kim[c], Byoung Koun Min[a,*]

[a] Clean Energy Center, Korea Institute of Science and Technology, 39-1 Hawolgok-dong, Seongbuk-gu, Seoul 136-791, Republic of Korea
[b] Photovoltaic Research Center, Korea Institute of Energy Research, 71-2 Jang-dong, Yuesong-gu, Daejeon 305-343, Republic of Korea
[c] Department of Chemical and Biomolecular Engineering, Yonsei University, 262 Seongsanno, Seodaemun-gu, Seoul 120-749, Republic of Korea

ARTICLE INFO

Article history:
Received 13 May 2010
Received in revised form 13 July 2010
Accepted 13 July 2010
Available online 23 July 2010

Keywords:
CIGS
$CuIn_xGa_{1-x}Se_2$
Quaternary
Binary

ABSTRACT

A chalcogenide quaternary crystal (CIGS) composed of Cu, In, Ga, and Se was synthesized by a solution reaction of Cu, In, and Ga nitrate and Se chloride in organic solvent, followed by an annealing process. In our synthetic method, the binary crystal of CuCl was found to be initially formed during the solution reaction at 130 °C for 3 h, but it turned into another binary crystal structure, β-CuSe at the longer time reaction (>12 h). The binary crystalline structure was then turned into quaternary crystal due to the heat treatment at 450 °C in reduction conditions and in the absence of additional elemental sources of In and/or Ga. For potential solar cell applications, the powder was also applied to prepare CIGS film by a paste coating. The structural characteristics of the powder and film were investigated by X-ray diffraction (XRD), transmission electron microscopy (TEM), selected area electronic diffraction (SAED), and scanning electron microscopy (SEM).

1. Introduction

A $CuIn_xGa_{1-x}Se_2$ (CIGS), a representative quaternary chalcogenide compound, has been admitted to be the most promising absorber material for thin film solar cell applications. For example, CIGS is a semiconductor material that has direct band gap and high absorption coefficient [1]. It was also known not to suffer from light induced degradation [1]. More importantly, the band gap of these materials can be controlled by changing the composition of each component [1,2]. The band gap of $CuInSe_2$ is known to be 1.04 eV, and it can be increased up to 1.7 eV when all In are replaced by Ga ($CuGaSe_2$).

Particularly for solar cell applications, the CIGS has been generally synthesized as a thin film by vacuum based deposition methods such as co-evaporation or sputtering. As noted by many other researchers, however, the current vacuum based processes have several drawbacks regarding manufacturing costs as well as efficiency of resource material use [3,4]. For example, the vacuum based processes require a high initial capital investment and maintenance capital expenses due to the necessity of the vacuum equipment. Moreover, the resource material loss was known to be significant, which again induces the increase of the manufacturing cost [3].

To solve the problems of the current CIGS thin film synthetic methods, non-vacuum processes have been suggested, which include printing, electroplating, spraying, paste coating, etc. [5–8]. Particularly, the particulate materials based paste coating, e.g. screen printing and doctor-blade coating, would be promising in terms of processing capital costs, efficiency of resource material usage, and processing speed [3,9]. Furthermore, these methods can be applied to continuous roll-to-roll depositing processes as well as large scale panel fabrications.

In order to fabricate the CIGS thin films by the particulate materials based printing methods, CIG oxide particles were first prepared and then applied to the paste coating followed by selenization with H_2Se gas [4]. Due to the concern of using highly toxic H_2Se gas, however, the direct application of the quaternary chalcogenide particles containing four elements (Cu, In, Ga, and Se) would be more favorable. For this purpose, many studies have been carried out in the way of applying nano-sized CIGS particles since it is useful to achieve very high packing density of the coated film. Most recently, Panthani et al. have developed the synthetic method of CIGS nanoparticles where the reaction was carried out at 240 °C in oleylamine [10]. Ternary compound ($CuInSe_2$) was also synthesized at the reaction temperature of 250 °C using tri-*n*-octylphosphine oxide (TOPO) [11]. Xiao et al. have synthesized $CuIn(Se_xS_{1-x})_2$ nanocystallites at 180 °C using an autoclave in etheylenediamine [12].

In general, however, CIGS thin film solar cells fabricated by a paste coating using nano-sized CIGS particles did not show high

* Corresponding author. Tel.: +82 2 958 5853; fax: +82 2 958 5809.
E-mail address: bkmin@kist.re.kr (B.K. Min).

0925-8388/$ – see front matter © 2010 Elsevier B.V. All rights reserved.
doi:10.1016/j.jallcom.2010.07.131

efficiency compared to those fabricated by vacuum based deposition methods. Among the many possible reasons for that, the limitation of crystal growth in CIGS layer would be a key factor since the presence of small grains induces high density of grain boundaries which may be served as recombination centers [13]. To overcome this problem, the use of submicron sized CIGS particles was considered rather than the nano-sized one for the preparation of CIGS pastes [5,9].

Herein, we suggested a simple synthetic method for the CIGS powders, which the size ranges up to a few hundred nanometers. In this study, we focused particularly on the crystal structure changes with respect to the heating temperature during the synthesis of CIGS alloy.

2. Experimental

A precursor mixture was prepared by dissolving the appropriate amounts of $Cu(NO_3)_2{\cdot}3H_2O$ (99.5%, Junsei, 0.504 g), $In(NO_3)_3{\cdot}xH_2O$ (99.99%, Alfa Aesar, 0.313 g), $Ga(NO_3)_3{\cdot}xH_2O$ (99.9%, Alfa Aesar, 0.266 g), and $SeCl_4$ (99.5%, Alfa Aesar, 0.917 g) in 1-propanol (99.5+%, Aldrich, 13 mL), followed by an addition of m-Xylene (99+%, Aldrich, 30 mL). Before refluxing the mixture solution, it was heated up to 130 °C to remove the alcohol. After the reaction for a certain time under Ar atmosphere, the precipitates were filtered and washed with xylene, propanol, and acetone several times. The precipitate was then annealed at 250 and 450 °C for 30 min in air and in H_2(5%)/Ar environment, respectively with a flow rate of 300 mL/min.

To prepare a paste the powder synthesized was dispersed in ethanol by an ultrasonic followed by the addition of terpineol (Fruka, 3.5 g) and ethyl cellulose (Alfa aesar, 0.1 g) to make rheological properties suitable for a doctor-blade coating or a spin coating. After coating the paste on the glass substrate, the sample was annealed at 450 °C for 30 min in a H_2S(1000 ppm)/Ar gas mixture at a flow rate of 100 mL/min.

Structural characterization of the powder and film was carried out using various analysis tools such as a transmittance electron microscopy (TEM, FEI Co., Tecnai F20), a scanning electron microscopy (SEM, Hitachi, S-4200), and a X-ray diffraction (XRD, Shimadzu, XRD-6000).

3. Results and discussion

For the synthesis of CIGS powders, the Cu, In, and Ga nitrate precursors were first dissolved in 1-propanol followed by the addition of xylene. In order to perform the reaction at a higher temperature (e.g. 130 °C) than the boiling point of 1-propanol, the alcohol was removed prior to the reflux. However, the use of alcohol was necessary because the precursors were not completely dissolved in aprotic organic solvent (e.g. xylene). Alternatively, the alcohol may play a role as a reducing agent similar to the polyol process, which is well known in metal nanoparticle synthesis [14,15]. In our particular synthetic procedure, a cationic Se precursor, $SeCl_4$, was used; therefore, a reduction process is needed to change the oxidation state of Se from +4 to −2. Propanol may be coordinated with Se^{4+} ions to form $Se(OC_3H_7)_4$,which is participated in the reaction with other ions.

Fig. 1 shows the XRD patterns of the precipitates obtained after the reaction at 130 °C. After the 3 h reaction, the sample revealed three apparent XRD peaks at 28.6°, 47.5°, and 56.2° 2θ. Based on the XRD database (JCPDS # 27-0184), the XRD peaks can be assigned to the (1 1 1), (2 2 0), and (3 1 1) phase of crystal structure of CuCl, respectively. The formation of CuCl crystal seems to have resulted from the generation of chlorine ions from the $SeCl_4$, which was used as a Se precursor. The longer reaction at the same temperature, however, resulted in a very different XRD pattern as seen in Fig. 1b. It became more complex, and its intensity was significantly diminished after the longer time reaction (24 h). Furthermore, the small XRD peaks are completely different from those of CuCl, implying that the crystal structure of CuCl was destructed due to the longer reaction. Based on the XRD database (JCPDS # 77-2383), the XRD peaks correspond to those of the β-CuSe crystal structure. Notably, the XRD pattern was not changed any further up to the reaction time of 48 h.

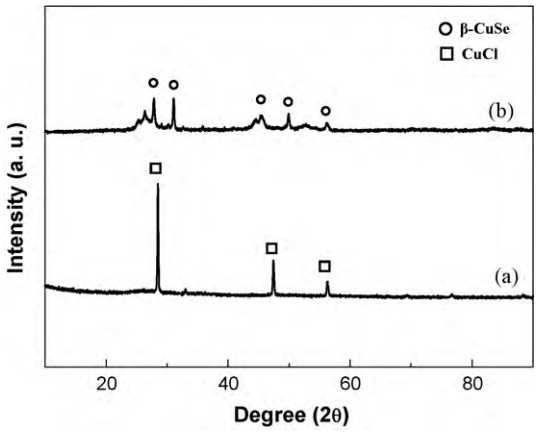

Fig. 1. X-ray diffraction (XRD) data of the precipitates obtained by the solution reaction at 130 °C for (a) 3 h and (b) 24 h.

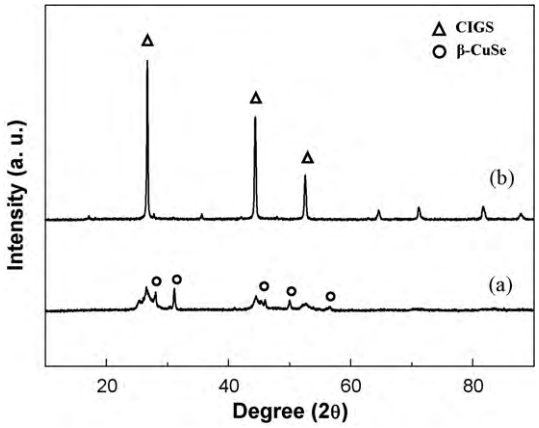

Fig. 2. X-ray diffraction (XRD) data of the powders prepared by annealing the precipitate at (a) 250 °C and (b) 450 °C under reduction conditions.

In order to prepare the crystalline CIGS particles, the precipitate obtained by the reaction for 24 h was annealed at two different temperatures of 250 and 450 °C in the reduction environment (H_2/Ar). Interestingly, there was little change in the XRD pattern (Fig. 2a) due to the annealing at 250 °C, indicating that there was no change in crystal structure of the powder. On the other hand, a dramatic change in the XRD pattern (Fig. 2b) occurred after the annealing at 450 °C, showing three distinct peaks at 26.7°, 44.4°, and 52.5° 2θ. In addition, the XRD peak intensity was enhanced by the factor of ~7, indicating an increase of crystallinity of the particles.

Based on the XRD database (JCPDS #35-1102) and other references, these peaks can be assigned to those of CIGS alloy [3,16]. The most intense peak at 26.7° 2θ represents the CIGS alloy with a (1 1 2) orientation. The other prominent peaks correspond to the (2 0 4)/(2 2 0) and (1 1 6)/(3 1 2) phase. In addition to these peaks commonly observed in CIGS, several weak peaks such as (4 0 0)/(0 0 8), (3 3 2)/(3 1 6) and (4 2 4)/(2 2 8) were also present in the XRD patterns.

The crystal structure of the powders was further confirmed by high resolution TEM images and corresponding selected area electronic diffraction (SAED) patterns as seen in Fig. 3. The TEM image of the sample corresponding to the XRD pattern of Fig. 1a showed small crystals (~5 nm), and its enlarged image (Fig. 3b) revealed atomic rows spaced about 0.312 nm, which is very close to those of CuCl. Both lattice structure and SAED pattern were substantially changed after the longer time reaction as seen in Fig. 3c and d. The spacing of the lattice fringes was estimated to be 0.337 nm, indicating that this crystallite is different from CuCl. SAED pattern

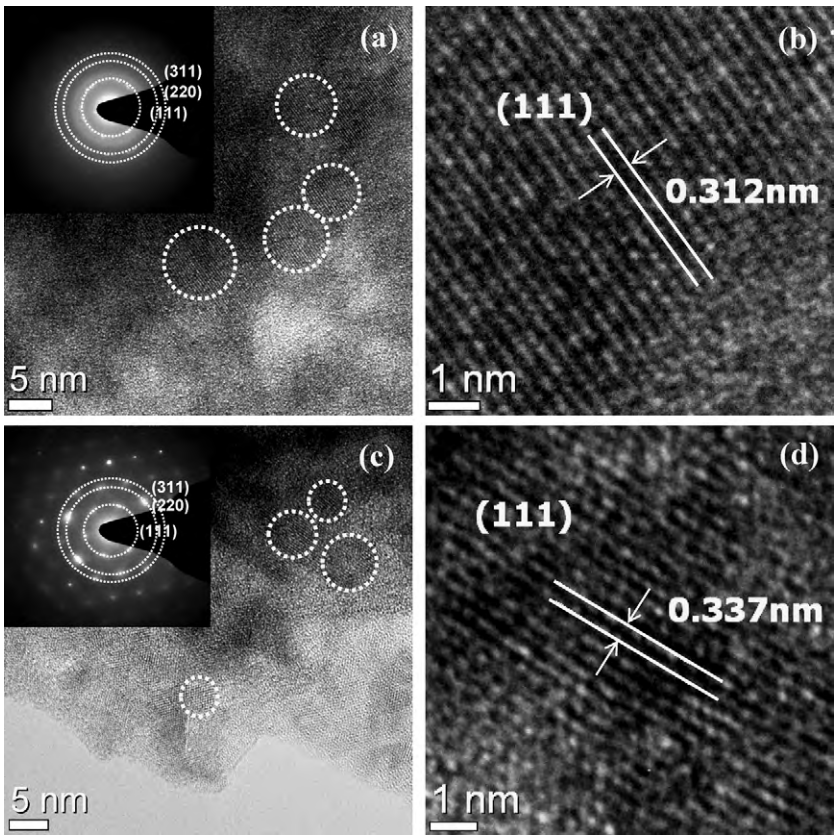

Fig. 3. Transmission electron microscopy (TEM) image of the precipitate obtained by the solution reaction at 130 °C for (a) and (b) 3 h and (c) and (d) 24 h. Insets of (a) and (c) are selected area electronic diffraction (SAED) patterns of the crystals marked by dotted circles. (b) and (c) are the enlarged image of the crystals showing lattice spaces.

showed apparent hexagonal spots, which was also different from that of CuCl. Both the lattice spacing and the SAED data were consistent with XRD data, confirming the formation of CuSe crystalline structure.

Consistent with the XRD data, the heat treatment at 250 °C did not substantially alter the crystal structure of CuSe (data not shown). The similar lattice spacing and SAED pattern to those of Fig. 3c and d were seen, implying that the binary crystal structure can persist up to this temperature. On the other hand, significant changes in the crystal structure were seen after the annealing at 450 °C as predicted in the XRD data. The general morphology observed in TEM images of CIGS powders is seen in Fig. 4, where relatively small crystals with size distribution from 10 to 50 nm seems to be deposited on large size grains (a few hundred nanometer scale). More importantly, however, both small and large grains have almost identical composition and lattice spacing based on SDX analysis as well as high resolution TEM (Fig. 4b), indicating that both are the same kind CIGS crystal. The SAED pattern also showed very sharp and strong spots (see inset of Fig. 4a), which is in agreement with the XRD data.

It is important to note here that the powder prepared by an annealing at 250 °C revealed the crystal structure of the binary compound, but it turned into quaternary crystal due to the annealing process at a higher temperature without adding any elemental sources. This result implies that there is an amorphous phase where In and Ga are incorporated as well as the binary crystal phase of

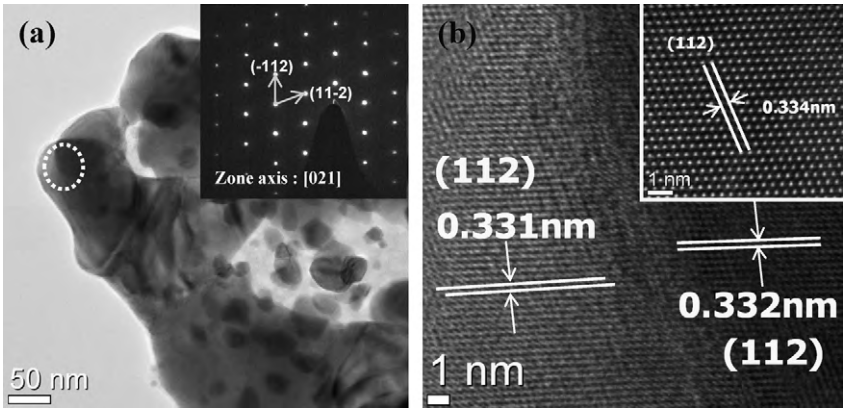

Fig. 4. (a) Transmission electron microscopy (TEM) image of the powder prepared by the annealing at 450 °C in reduction conditions from the precipitate, showing both small and large grains of CIGS. (b) The enlarged image of both small and large grains emphasizing same lattice spacing between them. Inset of (a) is a selected area electronic diffraction (SAED) pattern of the crystal, and inset of (b) is a high resolution TEM image of the area marked by dotted circles in (a).

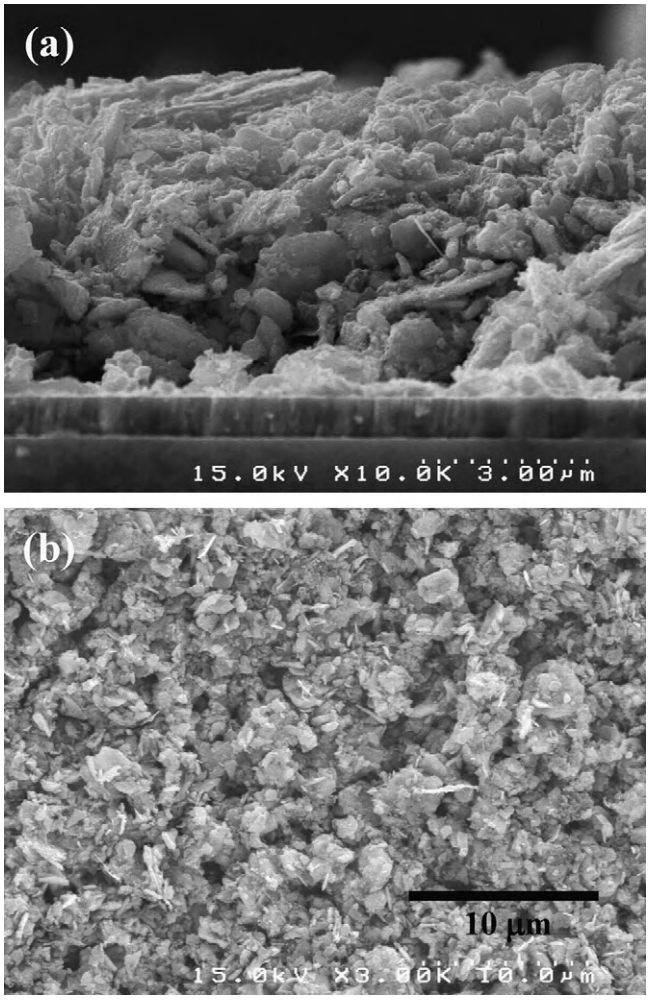

Fig. 5. (a) Cross-sectional and (b) planar SEM micrographs of CIGS thin film prepared by a paste coating using the powder synthesized.

CuSe in the powder prepared by the annealing at 250 °C. The heat treatment at higher temperature induced In, Ga, and residual Se to turn into the crystal structure.

Finally, the CIGS powder was applied to make CIGS film on molybdenum coated soda lime glass as seen in Fig. 5. In order to coat the film on glass substrate, a viscose paste with suitable rheological properties was first prepared. After a spin coating, the film was then annealed at two different successive conditions: 250 °C at ambient condition for 30 min and 450 °C at H_2S/Ar for 1 h. The first heat treatment at 250 °C was applied to remove residual organic solvent as well as binder as much as possible. The second annealing at 450 °C was also necessary to sinter the particles to form larger grains in the film. In addition, the heat treatment at H_2S/Ar conditions was found to provide some beneficial effects. This sulfurization led to the diminishing of residual carbon impurity. In addition, sulfur atoms inserted into the film during sulfurization can compensate for a little lack of selenium in CIGS powder we synthesized, which may enhance p-type characteristics of the CIGS film. Moreover, the adhesion of the film to Mo coated glass substrate was observed to be significantly enhanced due to the sulfurization process.

Even though the carbon impurities in the film were significantly diminished by sulfurization it would be necessary to almost completely remove the carbon residues in order to apply the CIGS thin films from the paste coating to the fabrication of CIGS solar cell devices. This may be achieved using organic binders that can be burned out at lower temperatures, which is currently being investigated in our laboratory.

4. Conclusions

High crystalline CIGS powder was synthesized by a solution reaction using volatile solvent at low temperature (130 °C), followed by annealing at elevated temperature (450 °C) in reduction conditions. We observed that the binary crystal structure was initially formed up to 250 °C and subsequently turned into quaternary crystal structure at higher temperature (450 °C), which was confirmed by both XRD and high resolution TEM analysis. Using this powder, CIGS film was prepared by a paste coating with sulfurization at 450 °C, which resulted in the enhancing of the adhesion between CIGS film and glass substrate and the diminishing of residual carbon impurity.

Acknowledgements

This work is supported by the Converging Research Center Program through the National Research Foundation of Korea (NRF-2009-0081910) and the National Research Foundation of Korea Grant (NRF-2009-C1AAA001-0092935) funded by the Ministry of Education, Science and Technology.

References

[1] M. Kemellm, M. Ritala, M. Keskela, Crit. Rev. Solid State Mater. Sci. 30 (2005) 1–31.
[2] P. Jackson, R. Würz, U. Rau, J. Mattheis, M. Kurth, T. Schlötzer, G. Bilger, J.H. Werner, Prog. Photovolt. Res. Appl. 15 (2007) 507–519.
[3] M. Kaelin, D. Rudmann, F. Kurdesau, H. Zogg, T. Meyer, A.N. Tiwari, Thin Solid Films 480–481 (2005) 486–490.
[4] V.K. Kapur, A. Bansal, P. Le, O.I. Asensio, Thin Solid Films 431–432 (2003) 53–57.
[5] C. Eberspacher, C. Fredric, K. Pauls, J. Serra, Thin Solid Films 387 (2001) 18–22.
[6] S.J. Ahn, C.W. Kim, J.H. Yun, J.C. Lee, K.H. Yoon, Sol. Energy Mater. Sol. Cells 91 (2007) 1836–1841.
[7] S.J. Ahn, K.H. Kim, Y.G. Chun, K.H. Yoon, Thin Solid Films 515 (2007) 4036–4040.
[8] M. Ganchev, J. Kois, M. Kaelin, S. Bereznev, E. Tzvetkova, O. Volobujeva, N. Stratieva, A. Tiwari, Thin Solid Films 511–512 (2006) 325–327.
[9] M. Kaelin, D. Rudmann, A.N. Tiwari, Sol. Energy 77 (2004) 749–756.
[10] M.G. Panthani, V. Akhavan, B. Goodfellow, J.P. Schmidtke, K. Dunn, A. Dodabalapur, P.F. Barbara, B.A. Korgel, J. Am. Chem. Soc. 130 (2008) 16770–16777.
[11] M.A. Malik, P. O'Brien, N. Revaprasadu, Adv. Mater. 11 (1999) 1441–1444.
[12] J. Xiao, Y. Xiong, R. Tang, Y. Qian, J. Mater. Chem. 11 (2001) 1417–1420.
[13] D.B. Mitzi, M. Yuan, W. Liu, A.J. Kellock, S.J. Chey, V. Deline, A.G. Schrott, Adv. Mater. 20 (2008) 3657–3662.
[14] B. Blin, F. Fievet, D. Beaupere, M. Figlarz, New J. Chem. 13 (1989) 67–72.
[15] J. Sun, Y. Jing, Y. Jia, M. Tillard, C. Belin, Mater. Lett. 59 (2005) 3933–3936.
[16] M.A. Contreras, M.J. Romero, R. Noufi, Thin Solid Films 511–512 (2006) 51–54.